# SHRIMP zircon U–Pb age constraints on Neoproterozoic Quruqtagh diamictites in NW China

Bei Xu, Shuhai Xiao, Haibo Zou, Yan Chen, Zheng-Xiang Li, Biao Song, Dunyi Liu, Chuanming Zhou, Xunlai Yuan

# SHRIMP zircon U–Pb age constraints on Neoproterozoic Quruqtagh diamictites in NW China

Bei Xu[a,*], Shuhai Xiao[b], Haibo Zou[c], Yan Chen [d], Zheng-Xiang Li[e], Biao Song[f], Dunyi Liu[f], Chuanming Zhou[g] and Xunlai Yuan[g]

[a]The Key Laboratory of Orogenic Belts and Crustal Evolution, Ministry of Education, Peking University, Beijing, 100871, China

[b]Department of Geosciences, Virginia Polytechnic Institute, Blacksburg, VA 24061, USA

[c]Department of Geology and Geography, Auburn University, Auburn, AL 36849, USA

[d]ISTO, Department of Geosciences, Orleans University, Orleans, 45067, France

[e]The Institute of Geoscience Research, Department of Applied Geology, Curtin University of Technology, GPO Box U1987, Perth, WA 6845, Australia

[f]Beijing SHRIMP Center, Institute of Geology, CAGS, Beijing, 100037, China

[g]State Key Laboratory of Paleontology and Stratigraphy, Nanjing Institute of Geology and Paleontology, Nanjing 210008, China

## Abstract

The Neoproterozoic Quruqtagh Group in the Tarim Block, NW China, contains multiple diamictites in the Bayisi, Altungol, Tereeken, and Hankalchough formations. These diamictites may represent three or possibly four discrete glaciations, although evidence for a glacial origin of the Bayisi and Altungol diamictite is ambiguous. To constrain their age and duration, we dated three volcanic beds (V1, V2, and V3) in the Quruqtagh Group using the SHRIMP (sensitive high-resolution ion microprobe) zircon U–Pb method. Volcanic bed V1 near the base of the Bayisi diamictite yields a 740 ± 7 Ma age, volcanic bed V2 near the top of the Bayisi Formation gives a 725 ± 10 Ma age, and volcanic bed V3 between the Tereeken and Hankalchough diamictites yields a 615 ± 6 Ma age. V1 and V2 have overlapping ages, and together these dates suggest that the Bayisi diamictite was deposited at around 730 Ma. The Tereeken and Altungol diamictites were deposited between 725 ± 10 Ma and 615 ± 6 Ma, and the Hankalchough diamictite between 615 ± 6 Ma and ~542 Ma (i.e., the Neoproterozoic–Cambrian transition). These dates and previously published chemostratigraphic data are consistent with (but doe not require) the correlation of the Tereeken and Hankalchough diamictites with the 635 Ma Nantuo and 582 Ma Gaskiers glaciations, respectively. However, the new dates are inconsistent with a single and globally synchronous Sturtian glaciation that occurred in the pre-Nantuo Neoproterozoic Era. Instead, currently available data necessitate that either multiple glaciations occurred, or a globally diachronous glacial event developed during a protracted period between ~750 Ma and ~650 Ma.

**Keywords:** SHRIMP geochronology; Quruqtagh Group; Neoproterozoic glaciation; Tarim; Northwest China

## 1. Introduction

The middle Neoproterozoic Era is characterized by repeated glaciations (Hoffman et al., 1998b), some of which may have reached tropical latitudes (Evans, 2000). However, the number, duration, synchroneity, extent, causes, and consequences of these glaciations are controversial ([Kaufman et al., 1997], [Kennedy et al., 1998], [Hoffman and Schrag, 2002] and [Jiang et al., 2003]), mostly because of relatively poor age constraints on many Neoproterozoic successions. On the basis of $\delta^{13}C$ chemostratigraphic correlation, Kaufman et al. (1997) proposed that there may have been four or more ice ages in the Neoproterozoic. This inference has been disputed by Kennedy et al. (1998) who argued that only two Neoproterozoic glaciations – the older Sturtian and the younger Marinoan (= Elatina) ice ages – are necessary to account for the diversity of cap carbonate lithostratigraphic and $\delta^{13}C$ chemostratigraphic features. Subsequent geochronological and stratigraphic data (Bowring et al., 2003), however, require at least three discrete Neoproterozoic glaciations—the Sturtian, the Elatina, and the Gaskiers glaciations ([Xiao et al., 2004], [Halverson, 2006] and [McCay et al., 2006]). Recent geochronological data suggest that the Sturtian glaciation in Australia and its supposed equivalents in Laurentia are younger than previously thought ([Lund et al., 2003], [Fanning and Link, 2004], [Fanning and Link, 2006] and [Kendall et al., 2006]), whereas the Kaigas glaciation in the Kalahari Craton does not temporally overlap with the Sturtian glaciation (Frimmel et al., 1996). These geochronological data require at least four Neoproterozoic glaciation—the Kaigas, Sturtian, Elatina, and Gaskiers, in geochronological order ([Hoffman and Schrag, 2002] and [Hoffmann et al., 2004]), or alternatively a pre-Elatina glaciation that is both diachronous and long-lasting. To provide new insights into the timing and duration of Neoproterozoic glaciations, we report new U–Pb SHRIMP ages from the Quruqtagh Group in NW China where four diamictite intervals have been described ([Xu et al., 2003] and [Xiao et al., 2004]). These new data help to constrain the age of the Quruqtagh diamictites and contribute to the global complexity of Neoproterozoic glaciations.

## 2. Geological setting and sampling

The Quruqtagh area is located in the southern foothills of the eastern Tianshan (inset in Fig. 1a), a major orogenic belt in central Asia separating the Tarim Block to the south from the Kazakhstan and Junggar blocks to the north. It is presently bounded by a major Paleozoic suture to the north and a Cenozoic thrust belt to the south, but stratigraphic correlations suggest it was part of the Tarim Block during the Neoproterozoic–Palaeozoic time (Gao et al., 1980). Regionally, the Neoproterozoic Quruqtagh Group overlies the Mesoproterozoic to early Neoproterozoic Paergangtage Group that consists of low-grade metamorphic rocks, including phyllites and carbonates with abundant columnar stromatolites. It underlies, probably disconformably, cherts and phosphorites of the Xishanblaq Formation that contains abundant basal Cambrian acritarchs and small shelly fossils (Yao et al., 2005).

The Quruqtagh Group crops out in the Xishankou, Mochia-khutuk, Yukkengol, and Xinger areas (Fig. 1a). The lower Quruqtagh Group is divided into the Bayisi, Zhaobishan, Altungol, and Tereeken formations, whereas the upper Quruqtagh Group consists of the Zhamoketi, Yukkengol, Shuiquan and Hankalchough formations (Fig. 1b). Thick diamictites occur in the Bayisi, Tereeken, and Hankalchough formations, and minor diamictites also occur in the Altungol Formation (Xiao et al., 2004). A glacial origin has been suggested for these diamictite intervals ([Gao and Zhu, 1984] and [Gao and Qian, 1985]). However, the most convincing evidence for a glacial origin comes from the Tereeken and Hankalchough

diamictites that contains abundant dropstones and striated clasts, and the glaciogenicity of the Altungol and Bayisi diamictite is still ambiguous (Xiao et al., 2004).

The Bayisi Formation consists of phyllite-slate grade metasediments and metavolcaniclastics. It is >250-m thick at Xishankou where four units of greenish gray diamictite are separated by quartz and polylithic metawackes. The thickness of the diamictite units varies from a few meters to more than 100 m. Outsized clasts, mostly derived from older metamorphic and igneous rocks, are set in silty and muddy matrix of the diamictite (Fig. 2a). Volcanic units occur at the base of the Bayisi Formation at Xinger (V1; Fig. 2e) and the top of the Bayisi Formation at Xishankou and Xinger (V2; Fig. 2f). The Bayisi diamictites are separated from the Altungol diamictite by the 100–300-m thick Zhaobishan Formation, which consists of metawackes, metarenites, calcareous siltstones, and slates. Altungol diamictites are also metamorphosed and deformed. Dolostones (with $\delta^{13}C$ values between 2‰ and 10‰; Fig. 1b) and interbeded volcanics occur over a 50-m interval in the upper Altungol Formation at

Xishankou. The overlying 200-m thick Tereeken Formation is less metamorphosed and consists of at least five diamictite units separated by finely laminated siltstones and mudstones. Abundant dropstones and striated clasts occur in the Tereeken diamictites (Fig. 2b).

The Tereeken Formation is succeeded by a 3–10-m thick cap carbonate in the basal Zhamoketi Formation (Fig. 2c). The Zhamoketi cap carbonate is characterized by negative $\delta^{13}C_{carb}$ values (Fig. 1b; Xiao et al., 2004) and positive $\delta^{34}S_{pyrite}$ values that are often greater than corresponding $\delta^{34}S_{carbonate\ associated\ sulfate}$ values (Shen et al., 2008). The rest of the Zhamoketi Formation and the overlying Yukkengol Formation consist of ~1200 m of meter-scale cycles of sandstone and siltstone, which are interpreted as deep-water turbidites. The Zhamoketi and Yukkengol formations are demarcated by 80–330 m of basaltic and andesitic volcanic rocks (V3; Fig. 2g), which are traditionally regarded as part of the uppermost Zhamoketi Formation. Further upsection is the Shuiquan Formation that consists of <100 m dolostone characterized by a large $\delta^{13}C$ shift from −9‰ to nearly 0‰ (Fig. 1b; Xiao et al., 2004). The uppermost Quruqtagh Group is represented by the Hankalchough Formation, which consists of ca. 400-m thick, light gray diamictite with abundant dropstones (Fig. 2d). The Hankalchough diamictite is succeeded by a 1–5-m thick dolostone characterized by variably negative $\delta^{13}C$ values, which is regarded as the Hankalchough cap carbonate (Fig. 1b; Xiao et al., 2004).

Samples were collected from three volcanic intervals (V1, V2, and V3) in the Bayisi and Zhamoketi formations (sample localities in Fig. 1a). Sample Xb006 came from V1 in the Xinger area, where the Bayisi Formation is 336-m thick and consists of diamictites as well as bi-modal basaltic, dacitic, and felsic lavas and pyroclastic rocks, with felsic lavas being the dominant (~75%) lithology (Xu et al., 2005). At the sample locality (GPS reading 41°27′12″N and 88°35′47″E, Fig. 2e), V1 consists of two basaltic beds overlain by three felsic beds and then diamictite. Sample Xb006 was collected from the lowest felsic bed. Sample A03112 was collected from V2 in the Xishankou area (GPS reading 41°35.32′N and 86°32.77′E), where a unit of ~50–200 m dark gray to purple andesitic to basaltic rocks occurs near the top Bayisi Formation (Fig. 2f). Bayisi diamictites occur mostly below V2, although a thin diamictite unit also occurs above V2. Sample 2371D was collected from V3 in the uppermost Zhamoketi Formation at Mochia-Khutuk (GPS reading 41°27′27″N and 87°52′51″E), where this volcanic interval consists of 80–330-m thick basaltic and andesitic lavas and pyroclastic rocks. The sample came from the middle part of an andesitic lava in V3 (Fig. 2g).

## 3. Geochronology

Zircons were separated from samples (Xb006, A03112, and 2371D) according to magnetic properties and density and hand picked for analysis. Xb006 and 2371D zircons were analyzed using the standard TEMORA (417 Ma, $^{206}Pb/^{238}U = 0.0668$), and A03112 zircons with the standard CZ3 (561.5 Ma, $^{206}Pb^*/^{238}U = 0.0914$, Kennedy personal communication May 2008). Sample and standard zircons were cast in an epoxy mount and polished down to half section. Cathodoluminescence imaging (Fig. 2h and i), carried out on electron microscopes at Department of Electronics of Peking University and Curtin University of Technology, was used to guide SHRIMP analyses.

Samples Xb006 and 2371D were analyzed on the Beijing SHRIMP II at the Chinese Academy of Geosciences, Ministry of Land and Resource, People's Republic of China. Procedures for zircon analysis of SHRIMP followed Compston et al. (1992) and Williams and Claesson (1987) with seven-scan duty cycles. Sample A03112 was analyzed using the SHRIMP II(B) at Curtin University of Technology with 6-scan duty cycles. Analytical spots of 25–30 μm diameters were used in both laboratories. The analytical data are listed in Table 1, Table 2 and Table 3 where errors on individual analysis are quoted at $2\sigma$ level based on both counting statistics errors (in $2\sigma$) and the mean of the standard measurements (in $2\sigma$; see calculation method in the footnotes of the tables). The software packages of Ludwig SQUID1.0 and ISOPLOT ([Ludwig, 2001a] and [Ludwig, 2001b]) were used for data reduction. Weighted mean ages are quoted at 95% confidence levels. The initial lead component was corrected using measured $^{204}Pb$.

Zircons from sample Xb006 are up to ~150 μm in lengths, and are euhedral with clear polygonal zoning that is indicative of magmatic origin. Fifteen spots on 13 zircon grains were analyzed. Isotopic data are shown in Table 1 and concordia plot in Fig. 3a. The $^{206}Pb/^{238}U$ ages of 11 analyses are assumed to belong to a single population with normally distributed uncertainties, producing a weighted mean age of 740 ± 7 Ma with a MSWD of 1.6 (Fig. 3a). Three slightly older analyses (Xb006-1.1 = 773 Ma, Xb006-2.1 = 792 Ma, Xb006-10.1 = 785 Ma) are distinct from the main population and were excluded from the mean calculation. In addition, analysis Xb006-3.1 gave an age of 2035 Ma, suggesting a likely detrital origin. We thus conclude that the best-estimated crystallisation age for Xb006 is 740 ± 7 Ma.

A previous SHRIMP analysis of zircons from sample Xb006 (V1) gave an age of 755 ± 15 Ma ($n$ = 10; MSWD = 1.50) (Xu et al., 2005). The age reported in this paper, 740 ± 7 Ma, is indistinguishable within analytical uncertainty from the previously reported age but with a much better precision.

Zircons separated from sample A03112 are up to ~150 μm in lengths, and euhedral with clear polygonal zoning that is indicative of magmatic zircons. Twenty zircon grains were analyzed. Isotopic data and concordia are shown in Table 2 and Fig. 3b, respectively. Excluding two discordant analyses (A03112.7-1 and A03112.11-1), one being an inherent core and the other showing apparent lead losses, the $^{206}Pb/^{238}U$ ages of the remaining 18 analyses are assumed to belong to a single population with normally distributed uncertainties. They yield a weighted-mean $^{206}Pb/^{238}U$ age of 725 ± 10 Ma, with a MSWD of 1.4. We regard this age as the best estimation of crystallisation age for sample A03112.

Zircons separated from sample 2371D are up to ~150 μm in lengths. Eighteen spots on 13 zircon grains were analyzed. Isotopic data and concordia plot are shown in Table 3 and Fig. 3c, respectively. Excluding three discordant analyses (2371D-10.1, 2371D-11.1 and 2371D-12.1), 15 analyses on 10 zircons yield a weighted-mean $^{206}Pb/^{238}U$ age of 615 ± 6 Ma (this error of ±6 Ma with a 95% confidence increases to ±7 Ma if we add in the 2$\sigma$ error of the standard measurement again), with a MSWD of 1.40. 2371D-10.1, 2371D-11.1 and 2371D-12.1 have ages ranging from ~1655 Ma to ~1816 Ma (Table 3), distinctly older than that of the main group, suggesting a detrital origin. We thus conclude that the best estimated age for 2371D is 615 ± 6 Ma.

## 4. Discussion

There is strong evidence (e.g., drop stones and striated clasts) suggesting that the Tereeken and Hankalcough diamicites are glaciogenic ([Gao et al., 1980], [Zhao et al., 1980], [Gao and Zhu, 1984] and [Xiao et al., 2004]), whereas evidence for a glacial origin of the Bayisi and Altungol diamictites is less convincing. The geochronometric data reported here provide new age constraints on the Quruqtagh diamictites. Given the stratigraphic proximity of the V1 and V2 volcanics to the basal and top Baiyisi diamictites, respectively, the 740 ± 7 Ma (V1) and 725 ± 10 Ma (V2) ages may be used to approximate the depositional age of the multiple diamictite beds within the Bayisi Formation. However, the difference between the two ages is insignificant given the analytical errors (see Fig. 3d). The overlap between the two ages becomes even greater when adding the 2$\sigma$ errors of the standard measurements, at 0.84% for the older age and 2.26% for the younger one, making them 740 ± 8 Ma (V1) and 725 ± 13 Ma (V2), respectively. We conclude that the accuracy of the current data is inadequate for defining the duration of the glacial event.

If the Bayisi diamictite beds represent a glaciation, then this glaciation may have occurred between 740 ± 7 Ma and 725 ± 10 Ma. Diamictites in the Altungol and Tereeken formations must have been deposited between 725 ± 10 Ma and 615 ± 6 Ma, and the Hankalchough diamictites between 615 ± 6 Ma and ~542 Ma—the best age estimate of the Ediacaran–Cambrian boundary (Amthor et al., 2003). Pending on further verification of the glacial origin of the Bayisi and Altungol diamictites, the Quruqtagh ages may contribute new insights into the geochronology and global correlation of Neoproterozoic glacial deposits (Table 4; Fig. 4).

### 4.1. Correlation of the Bayisi diamictite

The Bayisi diamictite has previously been interpreted as evidence of a Sturtian-age glaciation in the Quruqtagh area (Xiao et al., 2004). Traditionally, the Sturtian glaciation was believed to be ~723 Ma, on the basis of a U–Pb zircon age of 723 +16/−10 Ma from a tuffaceous bed near the base of the Ghubrah diamictite in Oman (Brasier et al., 2000), which was regarded as an equivalent of the Australian Sturtian glaciation. In addition, the 723 ± 7 Ma Franklin dikes share a similar paleopole position with the glaciogenic Sayunei Formation in Laurentia, which is thought to be another equivalent of the Sturtian glaciation (Heaman et al., 1992). Building

on the assumption that the Sturtian glaciation in South Australia – its type area – is also 723 Ma, many diamictites in other regions were regarded as Sturtian in age, often on weak geochronological grounds. This tends to inflate the definition of the Sturtian glaciation and confuse global correlation. In the following paragraphs, geochronological constraints on the "Sturtian" diamictites are reviewed in order to determine whether the Bayisi diamictite can be permissibly correlated with any of these "Sturtian" diamictites.

Recent data from South Australia – the type area for the Sturtian glaciation – suggest that the Sturtian glaciation is much younger than 723 Ma. Two recently published Re–Os ages (643.0 ± 2.4 Ma from black shales of the Tindelpina Member of South Australia and 657.2 ± 5.4 Ma from black shales of the Aralka Formation in central Australia) provide minimum age constraints for the Sturtian glaciation in Australia (Kendall et al., 2006). A vitreous tuffaceous bed in the upper unit of the Sturtian Merinjina Formation in South Australia gives a U–Pb SHRIMP age of ca. 658 Ma (Fanning and Link, 2006), indistinguishable from the Re–Os age from the Aralka Formation that is regarded as post-Sturtian deposits. Thus, the Sturtian glaciation in its type area may be as young as 658 Ma, and likely younger than the Bayisi diamictite.

Direct dating of Laurentia diamictites that are traditionally regarded as coeval to the Sturtian glaciation in South Australia also gives ages much younger than 723 Ma ([Lund et al., 2003] and [Fanning and Link, 2004]). A 717 ± 4 Ma age from a rhyolitic clast in the upper Scout Mountain diamictite in southeastern Idaho has been interpreted as representing the age of the Bannock Volcanic Member that underlies the Scout Mountain Member. This age potentially places a maximum age on the Scout Mountain diamictite—a possible Sturtian equivalent in Laurentia (Fanning and Link, 2004). In addition, a zircon U–Pb SHRIMP age of 709 ± 4 Ma from the Bancock Volcanic Member is interpreted as synglacial with the Scout Mountain diamictite (Fanning and Link, 2004). Furthermore, U–Pb SHRIMP zircon ages from rhyodacite flows in the upper Edwardsburg diamictite in central Idaho, also regarded as Sturtian age deposits, are 684 ± 4 Ma and 685 ± 7 Ma (Lund et al., 2003). These dates from Laurentia and South Australia suggest that a direct correlation between the Bayisi diamictite and the Sturtian diamictites in South Australia and Laurentia seems unlikely.

In Oman, the Ghubrah diamictite is regarded as equivalent to the Sturtian glaciation (Brasier et al., 2000). A tuffaceous bed near the base of the Ghubrah diamictite gave a zircon U–Pb age of 723 +16/−10 Ma (Brasier et al., 2000). However, subsequent analysis gave a more precise zircon U–Pb age of 711.5 ± 0.3 Ma ([Allen et al., 2002] and [Bowring et al., 2007]). These dates do not rule out a partial overlapping between the Bayisi and Ghubrah diamictites. However, considering that the 725 ± 10 Ma age came from near the top Bayisi diamictite whereas the 711.5 ± 0.3 Ma age came from the basal Ghubrah diamictite, it seems unlikely that these two diamictites are strictly coeval.

Neoproterozoic diamictites that are supposedly of Sturtian age also occur in South China, where there may be three Neoproterozoic diamictites—the Changan, Tiesiao, and Nantuo diamictites, in geochronological order (Zhou et al., 2004), although some geologists regard the Tiesiao diamictite as a lateral equivalent of the Changan diamictite (Liu, 1991). Regardless, the Changan diamictite is often regarded as Sturtian in age (Zhou et al., 2004). Tuffaceous deposits from successions underlying the Changan diamictite or interpreted to be older than the Changan diamictite have been dated using both SHRIMP and TIMS methods, giving zircon U–Pb ages of 761 ± 8 Ma (Li et al., 2003), 758 ± 23 Ma (Yin et al., 2003), and 748 ± 12 Ma (Ma et al., 1984). Less widely known is a zircon U–Pb age of 736 ± 2 Ma from the Banxi Group in Hunan Province, which is interpreted to be older than the Changan diamictite (Gan et al., 1993). These dates provide maximum constraints on the age of the Changan diamictite. At face value, these radiometric ages do not completely preclude a partial correlation between the Bayisi diamictite in Quruqtagh (740 ± 7 Ma and 725 ± 10 Ma) and the Changan diamictite in South China (<736 ± 2 Ma), although a strict correlation requires direct dating of the Changan diamictite.

Two Neoproterozoic diamictites occur in northern Namibia—the Chuos and Ghaub diamictites in geochronological order. The Chuos diamictite is interpreted to be of Sturtian age (Hoffman and Schrag, 2002) and has been dated to be <746 ± 2 Ma (Hoffman et al., 1996). Like the Bayisi–Changan correlation, the Bayisi–Chuos correlation is permissible but inconclusive.

Multiple Neoproterozoic diamictites also occur in southern Namibia and northwestern Zambia. The oldest diamictite in these areas appear to be older than the Sturtian diamictites in Australia and supposedly Sturtian-age diamictites in Laurentia, South China, Oman, and northern Namibia. For example, the Kaigas diamictite in the Gariep belt of southern Namibia has been constrained to be >741 ± 6 Ma (Frimmel et al., 1996), and diamictites in the Port Nolloth Group of southern Namibia has been constrained to be >752 ± 6 Ma (Borg et al., 2003). More recently, high-precision zircon U–Pb ages from rhyolites above and below the Kaigas diamictite in the Gariep belt of southern Namibia constrain its age to be ~754 Ma and its duration to be <2 myr (Hoffmann et al., 2006). Furthermore, Neoproterozoic glacial diamictite in the basal Ngubu Group (formerly lower Kundelungu Group) in northwestern Zambia has been constrained between 765 ± 5 Ma and 735 ± 5 Ma ([Key et al., 2001] and [Cailteux et al., 2005]). Although the significance of these African ages remains unclear because of the stratigraphic complexity of the African successions, it seems that these glaciations may have terminated before the Sturtian glaciation. Because the basal boundary of the Bayisi Formation is not geochronologically constrained (the 740 ± 7 Ma age is from within the Bayisi Formation), it is still possible that the Bayisi and Kaigas diamictites may partially overlap. However, a synchronous initiation and termination of these two diamictites can be ruled out.

To summarize, the correlation of the Bayisi diamictite with other Neoproterozoic diamictites is a challenge. Although the depositional age of the Bayisi diamictite may partially overlap with the Kaigas and supposedly Sturtian glaciations, it is unlikely that it was synchronous in both initiation and termination with either glaciation. Thus, it is possible that there may have been multiple regional glaciations between ~750 Ma and 650 Ma. Alternatively, the Bayisi diamictite, if it is indeed glaciogenic, may represent part of a protracted glaciation that started and ended diachronously in different regions.

## 4.2. Correlation of the Altungol diamictite

The glacial origin of the Altungol diamictite remains to be unambiguously verified. Nonetheless, its depositional age between 725 ± 10 Ma and 615 ± 6 Ma is consistent with a correlation with either the Sturtian or Elatina glaciation. Given that no cap carbonate is associated with the Altungol diamictite, we prefer the interpretation that the Altungol diamictite, if it is glaciogenic, and the Tereeken diamiacte collectively represent a single ice age (Xiao et al., 2004). This preferred correlation is also consistent with the highly positive $\delta^{13}C$ values (~10‰ PDB) in an underlying carbonate unit (Fig. 1b); such highly positive $\delta^{13}C$ values typically (although not exclusively) occur in carbonate successions between the Sturtian and Elatina glaciations (Halverson et al., 2005).

## 4.3. Correlation of the Tereeken glaciation

The Tereeken diamictite is unambiguously glaciogenic (Fig. 2b). On the basis of $\delta^{13}C$ chemostratigraphy of the overlying cap carbonate, previous investigators ([Xiao et al., 2004] and [Shen et al., 2008]) have argued that the Tereeken glaciation may be correlated with the

Elatina glaciation in Australia, Nantuo glaciation in South China, and the Ghaub glaciation in northern Namibia. The Nantuo and Ghaub glaciations are likely coeval and have been dated to be ~635 Ma ([Hoffmann et al., 2004] and [Condon et al., 2005]). The age of the Elatina glaciation in its type area has not been directly dated, and it is uncertain whether the <575 ± 3 Ma Cottons Breccia in Tasmania (Calver et al., 2004) can be correlated with the Elatina diamictite. However, chemostratigraphic correlation based on $\delta^{13}C$ and $^{87}Sr/^{86}Sr$ of cap carbonates suggests that the Elatina, Nantuo, and Ghaub glaciations may be synchronous ([Kennedy et al., 1998], [Halverson et al., 2007] and [Zhou and Xiao, 2007]). Combining the Re–Os ages from the Tindelpina Member in the Flinders Ranges and the zircon U–Pb ages from the Doushantuo cap carbonate atop the Nantuon diamictite in South China, a global Elatina-age glaciation is permissible between 643.0 ± 2.4 Ma (Kendall et al., 2006) and 635.2 ± 0.6 Ma (Condon et al., 2005). Diamictites in the Tereeken (and possibly Altungol) Formation, constrained between 725 ± 10 Ma and 615 ± 6 Ma, can thus be permissibly correlated with the Elatina glaciation. This correlation is further supported by sedimentary features and $\delta^{13}C$ profile of the Zhamokete cap carbonate atop the Tereeken diamictite, which shows a chemostratigraphic pattern similar to other cap carbonate to Elatina-age diamictites (Xiao et al., 2004).

## 4.4. Correlation of the Hankalchough glaciation

The youngest diamictite in the Quruqtagh Group – the Hankalchough diamictite – is also glaciogenic, supported by sedimentary evidence such as drop stones and striated clasts ([Zhao et al., 1980] and [Gao and Zhu, 1984]). Traditionally, the Hankalchough diamictite has been correlated with the Zhengmuguan diamictite in Ningxia (NW China) and the Hongtiegou diamictite in the Zhoujieshan area (NW China) ([Zhao et al., 1980] and [Lu et al., 1985]). The Hankalchough diamictite underlies phosphorites that contain basal Cambrian microfossils (Yao et al., 2005). The Zhengmuguan and Hongtiegou diamictites underlie siliciclastic rocks that contain late Ediacaran fossils such as *Palaeopascichnus* and *Shaanxilithes* (Shen et al., 2007); these genera occur in the 551–542 Ma Dengying Formation or its equivalents in South China ([Xing et al., 1984] and [Dong et al., 2008]). Thus, biostratigraphic data are consistent with an Ediacaran age for the Hankalchough, Zhengmuguan, and Hongtiegou diamictites. The radiometric ages reported here further constrain the Hankalchough glaciation between 615 ± 6 Ma and ~542 Ma. The new data are consistent with previous proposition (Xiao et al., 2004) that the Hankalchough glaciation may be correlated with the ~582 Ma Gaskiers glaciation in Newfoundland (Bowring et al., 2003), although it remains possible that multiple short-lived glaciations may have occurred in the Ediacaran Period.

## 5. Conclusions

Diamictites occur in the Bayisi, Altungol, Tereeken, and Hankalchough formations in the Neoproterozoic Quruqtagh Group in NW China. The Tereeken and Hankalchogh diamictites are unequivocally glaciogenic, although a glacial origin for the Bayisi and Altungol diamictites remains to be verified. New SHRIMP zircon U–Pb ages from three volcanic beds within the Quruqtagh Group suggest that the Bayisi diamictite was deposited around 730 Ma (740 ± 7 Ma and 725 ± 10 Ma), the Tereeken and Altungol diamictites between 725 ± 10 Ma and 615 ± 6 Ma, and the Hankalchough diamictite between 615 ± 6 Ma and ~542 Ma. These dates are consistent with the correlation of the Tereeken and Hankalchough diamictites with the 635 Ma Nantuo and the 582 Ma Gaskiers glaciations, respectively, although more precise age constraints are required to prove global synchroneity of the Nantuo and Gaskiers glaciations. Despite the new radiometric ages, the correlation of the Bayisi and Altungol

diamictites remains unresolved, and it is possible that multiple glaciations or a long-lasting but globally diachronous glaciation may have occurred between ~750 Ma and ~650 Ma.

## Acknowledgments

We are grateful to Y. Li, H. Bao, and H. Wang for field assistance. We would like to thank S. Bowring, D. Condon, G. Halverson, X. Dong, G. Shields, and Y.F. Zhu for useful discussion and comments. We benefited from very constructive reviews by Dan Condon and Bill Davis. This work was supported by the National Natural Science Foundation of China (40572133, 40032010) and CSC of China (2003811069), US National Science Foundation (EAR-0545135), Australian Research Council (DP0770228), and NASA Exobiology Program (NNG05GP21G). This is TIGeR publication No.154.

## References


Aleinikoff et al., 1995 J.N. Aleinikoff, R.E. Zartman, M. Walter, D.W. Rankin, P.T. Lyttle and W.C. Burton, U–Pb ages of metarhyolites of the Catoctin and Mount Rogers formations, central and southern Appalachians: evidence for 2 pulses of Iapetan rifting, *Am. J. Sci.* **295** (1995), pp. 428–454.

Allen et al., 2002 P.A. Allen, S.A. Bowring, J. Leather, M. Brasier, A. Cozzi, J.P. Grotzinger, G. McCarron and J. Amthor, Chronology of Neoproterozoic glaciations: new insights from Oman, *Proceedings of the 16th International Sedimentological Congress: Johannesburg, International Association of Sedimentologists, Abstract volume* (2002), pp. 7–8.

Amthor et al., 2003 J.E. Amthor, J.P. Grotzinger, S. Schröder, S.A. Bowring, J. Ramezani, M.W. Martin and A. Matter, Extinction of *Cloudina* and *Namacalathus* at the Precambrian–Cambrian boundary in Oman, *Geology* **31** (5) (2003), pp. 431–434

Barfod et al., 2002 G.H. Barfod, F. Albaréde, A.H. Knoll, S. Xiao, P. Télouk, R. Frei and J. Baker, New Lu–Hf and Pb–Pb age constraints on the earliest animal fossils, *Earth Planet. Sci. Lett.* **201** (2002), pp. 203–212.

Benus, 1988 A.P. Benus, Sedimentological context of a deep-water Ediacaran fauna (Mistaken Point Formation, Avalon Zone, eastern Newfoundland). In: E. Landing, G.M. Narbonne and P. Myrow, Editors, *Trace Fossils, Small Shelly Fossils and the Precambrian–Cambrian Boundary*, Bulletin of the New York State Museum (1988), pp. 8–9.

Borg et al., 2003 G. Borg, K. Kärner, M. Buxton, R. Armstrong and S.W.V.D. Merwe, Geology of the Skorpion supergene zinc deposit Southern Namibia, *Econ. Geol.* **98** (2003), pp. 749–771.

Bowring et al., 2003 S. Bowring, P. Myrow, E. Landing, J. Ramezani and J. Grotzinger, Geochronological constraints on terminal Neoproterozoic events and the rise of metazoans, *Geophys. Res. Abs.* **5** (2003), p. 13219.

Bowring et al., 2007 S.A. Bowring, J.P. Grotzinger, D.J. Condon, J. Ramezani, M.J. Newall and P.A. Allen, Geochronologic constraints on the chronostratigraphic framework of the Neoproterozoic Huqf Supergroup Sultanate of Oman, *Am. J. Sci.* **307** (2007), pp. 1097–1145.
Brasier et al., 2000 M. Brasier, G. McCarron, R. Tucker, J. Leather, P. Allen and G. Shields, New U–Pb zircon dates for the Neoproterozoic Ghubrah glaciation and for the top of the Huqf Supergroup, *Oman. Geol.* **28** (2) (2000), pp. 175–178.

Cailteux et al., 2005 J.L.H. Cailteux, A.B.H. Kampunzu and M.J. Batumike, Lithostratigraphic position and petrographic characteristics of R.A.T. ("Roches Argilo-Talqueuses") Subgroup, Neoproterozoic Katangan Belt (Congo), *J. Afr. Earth Sci.* **42** (2005), pp. 82–94.

Calver et al., 2004 C.R. Calver, L.P. Black, J.L. Everard and D.B. Seymour, U–Pb zircon age constraints on late Neoproterozoic glaciation in Tasmania, *Geology* **10** (2004), pp. 893–896.

Colpron et al., 2002 M. Colpron, J.M. Logan and J.K. Mortensen, U–Pb zircon age constraint for late Neoproterozoic rifting and initiation of the lower Paleozoic passive margin of western Laurentia, *Can. J. Earth Sci.* **39** (2002), pp. 133–143.

Compston et al., 1992 W. Compston, I.S. Williams, J.L. Kirschvink, Z. Zhang and G. Ma, Zircon U–Pb ages for the Early Cambrian time-scale., *J. Geol. Soc. Lond.* **149** (1992), pp. 171–184.

Compston et al., 2002 W. Compston, A.E. Wright and P. Toghill, Dating the late Precambrian volcanicity of England and Wales, *J. Geol. Soc. Lond.* **159** (2002), pp. 323–339.

Condon et al., 2005 D. Condon, M. Zhu, S. Bowring, W. Wang, A. Yang and Y. Jin, U–Pb ages from the Neoproterozoic Doushantuo Formation, *Chin. Sci.* **308** (2005), pp. 95–98

Dempster et al., 2002 T.J. Dempster, G. Rogers, P.W.G. Tanner, B.J. Bluck, R.J. Muir, S.D. Redwood, T.R. Ireland and B.A. Paterson, Timing of deposition, orogenesis and glaciation within the Dalradian rocks of Scotland: constraints from U–Pb zircon ages, *J. Geol. Soc. Lond.* **159** (2002), pp. 83–94

Dong et al., 2008 L. Dong, S. Xiao, B. Shen and C. Zhou, Silicified *Horodyskia* and *Palaeopascichnus* from upper Ediacaran cherts in South China: tentative phylogenetic interpretation and implications for evolutionary stasis, *J. Geol. Soc. Lond.* **165** (2008), pp. 365–378.

Evans, 2000 D.A.D. Evans, Stratigraphic, geochronological, and paleomagnetic constraints upon the Neoproterozoic climatic paradox, *Am. J. Sci.* **300** (5) (2000), pp. 347–433.

Evans et al., 1997 D.V.D. Evans, K. Lund, J.N. Aleinikoff and C.M. Fanning, SHRIMP U–Pb age of late Proterozoic volcanism in central Idaho, *Geol. Soc. Am. Abs. Programs* **29** (6) (1997), p. 196.

Fanning and Link, 2004 C.M. Fanning and P.K. Link, U–Pb SHRIMP ages of Neoproterozoic (Sturtian) glaciogenic Pocatello Formation, southeastern Idaho, *Geology* **32** (10) (2004), pp. 881–884.

Fanning and Link, 2006 C.M. Fanning and P.K. Link, Constraints on the timing of the Sturtian glaciation from southern Australia: i.e. for the true Sturtian GSA, *Annu. Meeting Abs. Prog.* **38** (7) (2006), p. 115.
Ferri et al., 1999 Ferri, F., Rees, C.J., Nelson, J.L., Legun, A.S., 1999. Geology and mineral deposits of the northern Kechika Trough between Gataga River and the 60th parallel. British Columbia Ministry of Energy and Mines, Bulletin 107, 1–122.

Fetter and Goldberg, 1995 A.H. Fetter and S.A. Goldberg, Age and geochemical characteristics of bimodal magmatism in the Neoproterozoic Grandfather Mountain rift basin, *J. Geol.* **103** (1995), pp. 313–326.

Frimmel et al., 1996 H.W. Frimmel, U.S. Klötzi and P.R. Siegfried, New Pb–Pb single zircon age constraints on the timing of Neoproterozoic glaciation and continental break-up in Namibia, *J. Geol.* **104** (1996), pp. 459–469.

Gan et al., 1993 X. Gan, F. Zhao, H. Li, X. Tang and J. Huang, Single zircon U–Pb age of the Banxi Group in Hunan Province (in Chinese), *Abstracts of the Fifth National Symposium on Isotopic Geochronology and Geochemistry* (1993), pp. 10–12.

Gao and Qian, 1985 Z. Gao and J. Qian, Sinian glacial deposits in Xinjiang, Northwest China, *Precambrian Res.* **29** (1–3) (1985), pp. 143–147.

Gao and Zhu, 1984 Z. Gao and S. Zhu, Precambrian Geology in Xinjiang China, Xinjiang People's Publishing House, Urumuqi, China (1984) 151 pp..

Gao et al., 1980 Gao, Z., Peng, C., Li, Y., Qian, J., Zhu, S., 1980. The Sinian System and its glacial deposits in Quruqtagh, Xinjiang. In: Tianjin Institute of Geology and Mineral Resources (Ed.), Research in Precambrian Geology, Sinian Suberathem in China. Tianjin Science and Technology Press, Tianjin, pp. 186–213.

Grotzinger et al., 1995 J.P. Grotzinger, S.A. Bowring, B.Z. Saylor and A.J. Kaufman, Biostratigraphic and geochronologic constraints on early animal evolution, *Science* **270** (1995), pp. 598–604.

Halverson, 2006 G. Halverson, A Neoproterozoic chronology. In: S. Xiao and A.J. Kaufman, Editors, *Neoproterozoic Geobiology*, Kluwer Academic Publishers, Dordrecht, the Netherlands (2006), pp. 172–231.

Halverson et al., 2005 G.P. Halverson, P.F. Hoffman, D.P. Schrag, A.C. Maloof and A.H.N. Rice, Toward a Neoproterozoic composite carbon-isotope record, *GSA Bull.* **117** (2005), pp. 1181–1207 doi: 10.1130/B25630.1.

Halverson et al., 2007 G.P. Halverson, F.O. Dudas, A. Maloof and S.A. Bowring, Evolution of $^{87}Sr/^{86}Sr$ composition of Neoproterozoic seawater, *Palaeogeogr. Palaeoclimatol. Palaeoecol.* **256** (2007), pp. 103–129.

Heaman et al., 1992 L.M. Heaman, A.N. LeCheminant and R.H. Rainbird, Nature and timing of Franklin igneous events Canada: implications for a Late Proterozoic mantle plume and the break-up of Laurentia, *Earth Planet. Sci. Lett.* **109** (1992), pp. 117–131.

Hoffman and Schrag, 2002 P.F. Hoffman and D.P. Schrag, The snowball Earth hypothesis: testing the limits of global change, *Terra Nova* **14** (2002), pp. 129–155.

Hoffman et al., 1996 P.F. Hoffman, D.P. Hawkins, C.E. Isachsen and S.A. Bowring, Precise U–Pb zircon ages for early Damaran magmatism in the Summas Mountains and Welwitschia Inlier, northern Damara belt Namibia, *Commun. Geol. Survey Namibia* **11** (1996), pp. 47–52.

Hoffman et al., 1998a P.F. Hoffman, A.J. Kaufman and G.P. Halverson, Comings and goings of global glaciations on a Neoproterozoic tropical platform in Namibia, *GSA Today* **8** (5) (1998), pp. 1–9.

Hoffman et al., 1998b P.F. Hoffman, A.J. Kaufman, G.P. Halverson and D.P. Schrag, A Neoproterozoic snowball Earth, *Science* **281** (1998), pp. 1342–1346.

Hoffmann et al., 2004 K.-H. Hoffmann, D.J. Condon, S.A. Bowring and J.L. Crowley, U–Pb zircon date from the Neoproterozoic Ghaub Formation Namibia: constraints on Marinoan glaciation, *Geology* **32** (2004), pp. 817–820.

Hoffmann et al., 2006 K.-H. Hoffmann, D.J. Condon, S.A. Bowring, A.R. Prave and A. Fallick, Lithostratigraphic, carbon ((13C) isotope and U–Pb zircon age constraints on early Neoproterozoic (ca. 755 Ma) glaciation in the Gariep Belt, southern Namibia, *Proceedings of the Snowball Earth Conference* July 16-21, 2006, Monte Verita, Ticino, Switzerland (2006), p. 51.

Jefferson and Parrish, 1989 C.W. Jefferson and R.R. Parrish, Late Proterozoic stratigraphy, U–Pb zircon ages, and rift tectonics, Mackenzie Mountains, northwestern Canada, *Can. J. Earth Sci.* **26** (1989), pp. 1784–1801.

Jiang et al., 2003 G. Jiang, M.J. Kennedy and N. Christie-Blick, Stable isotopic evidence for methane seeps in Neoproterozoic postglacial cap carbonates, *Nature* **426** (2003), pp. 822–826.

Karlstrom et al., 2000 K.E. Karlstrom, S.A. Bowring, C.M. Dehler, A.H. Knoll, S.M. Porter, D.J.D.B. Marais, A. Weil, Z.D. Sharp, J.W. Geissman, M.B. Elrick, J.M. Timmons, L.J. Crossey and K.L. Davidek, Chuar Group of the Grand Canyon: Record of breakup of Rodinia, associated change in the global carbon cycle, and ecosystem expansion by 740 Ma, *Geology* **28** (2000), pp. 619–622.

Kaufman et al., 1997 A.J. Kaufman, A.H. Knoll and G.M. Narbonne, Isotopes, ice ages, and terminal Proterozoic earth history, *Proc. Natl. Acad. Sci. U.S.A.* **94** (1997), pp. 6600–6605.

Kendall et al., 2004 B.S. Kendall, R.A. Creaser, G.M. Ross and D. Selby, Constraints on the timing of Marinoan "Snowball Earth" glaciation by $^{187}Re$–$^{187}Os$ dating of a Neoproterozoic, post-glacial black shale in Western Canada, *Earth Planet. Sci. Lett.* **222** (2004), pp. 729–740.

Kendall et al., 2006 B. Kendall, R.A. Creaser and D. Selby, Re–Os geochronology of postglacial black shales in Australia: constraints on the timing of "Sturtian" glaciation, *Geology* **34** (2006), pp. 729–732.

Kennedy et al., 1998 M.J. Kennedy, B. Runnegar, A.R. Prave, K.H. Hoffmann and M.A. Arthur, Two or four Neoproterozoic glaciations?, *Geology* **26** (12) (1998), pp. 1059–1063.

Key et al., 2001 R.M. Key, A.K. Liyungu, F.M. Njamu, V. Somwe, J. Banda, P.N. Mosley and R.A. Armstrong, The western arm of the Lufilian Arc in NW Zambia and its potential for copper mineralization, *J. Afr. Earth Sci.* **33** (2001), pp. 503–528.

Krogh et al., 1988 T.E. Krogh, D.F. Strong, S.J. O'Brien and V. Papezik, Precise U–Pb zircon dates from the Avalon Terrane in Newfoundland, *Can. J. Earth Sci.* **25** (1988), pp. 442–453.

Li et al., 2003 Z.X. Li, X.H. Li, P.D. Kinny, J. Wang, S. Zhang and H. Zhou, Geochronology of Neoproterozoic syn-rift magmatism in the Yangtze Craton South China and correlations with other continents: evidence for a mantle superplume that broke up Rodinia, *Precambrian Res.* **122** (1–4) (2003), pp. 85–109.

Link et al., 1993 Link, P.K., Christie-Blick, N., Devlin, W.J., Elston, D.P., Horodyski, R.J., Levy, M., Miller, J.M.G., Pearson, R.C., Prave, A., Stewart, J.H., Winston, D., Wright, L.A., Wrucke, C.T., 1993. Middle and late Proterozoic stratified rocks of the western U.S. Cordillera, Colorado Plateau, and Basin Range province. In: Reed, J.C., et al. (Eds.), The Geology of North America, pp. 463–595.

Liu, 1991 H. Liu, The Sinian System in China, Science Press, Beijing (1991) 388 pp..

Lu et al., 1985 S. Lu, G. Ma, Z. Gao and W. Lin, Sinian ice ages and glacial sedimentary facies-areas in China, *Precambrian Res.* **29** (1985), pp. 53–63.

Ludwig, 2001a Ludwig, K.R., 2001a. SQUID version 1.02: a geochronological Toolkit for Microsoft Excel. Berkley Geochronological Centre Special Publication no. 2, 1–19.

Ludwig, 2001b Ludwig, K.R., 2001b. Users manual for Isoplot/Ex rev. 2.49. Berkeley Geochronology Centre Special Publication no. 1a, 1–56.

Lund et al., 2003 K. Lund, J.N. Aleinikoff, K.V. Evans and C.M. Fanning, SHRIMP U–Pb geochronology of Neoproterozoic Windermere Supergroup, central Idaho: implications for rifting of western Laurentia and synchroneity of Sturtian glacial deposits, *GSA Bull.* **115** (3) (2003), pp. 349–372.

Ma et al., 1984 G. Ma, H. Lee and Z. Zhang, An investigation of the limits of the Sinian System in South China. Bulletin of the Yichang Institute of Geology and Mineral Resources, *Chin. Acad. Geol. Sci.* **8** (1984), pp. 1–29.

Martin et al., 2000 M.W. Martin, D.V. Grazhdankin, S.A. Bowring, D.A.D. Evans, M.A. Fedonkin and J.L. Kirschvink, Age of Neoproterozoic bilaterian body and trace fossils, White Sea Russia: implications for metazoan evolution, *Science* **288** (2000), pp. 841–845.

McCay et al., 2006 G.A. McCay, A.R. Prave, G.I. Alsop and A.E. Fallick, Glacial trinity: Neoproterozoic Earth history within the British–Irish Caledonides, *Geology* **34** (2006), pp. 909–912.

McDonough and Parrish, 1991 M.R. McDonough and R.R. Parrish, Proterozoic gneisses of the Malton Complex, near Valemount British Columbia: U–Pb ages and Nd isotopic signatures, *Can. J. Earth Sci.* **28** (1991), pp. 1202–1216.

Preiss, 2000 W.V. Preiss, The Adelaide Geosyncline of South Australia and its significance in Neoproterozoic continental reconstruction, *Precambrian Res.* **100** (2000), pp. 21–63 doi:10.1016/S0301-9268(99)00068-6.

Ross and Villeneuve, 1997 Ross, G.M., Villeneuve, M.E., 1997. U–Pb geochronology of stranger stones in Neoproterozoic diamictites, Canadian Cordillera: implications for provenance and age of deposition. Geological Survey of Canada, Current Research 1997-F, 141–155.

Schaefer and Burgess, 2003 B.F. Schaefer and J.M. Burgess, Re–Os isotopic age constraints on deposition in the Neoproterozoic Amadeus Basin: implications for the ‘Snowball Earth’, *J. Geol. Soc. Lond.* **160** (2003), pp. 825–828.

Semikhatov, 1991 M.A. Semikhatov, General Problems of Proterozoic Stratigraphy in the USSR. Soviet Science Review G, *Geology* **1** (1991), pp. 1–192.

Shen et al., 2007 B. Shen, S. Xiao, L. Dong, C. Zhou and J. Liu, Problematic macrofossils from Ediacaran successions in the North China and Chaidam blocks: implications for their evolutionary roots and biostratigraphic significance, *J. Paleontol.* **81** (2007), pp. 1396–1411.

Shen et al., 2008 B. Shen, S. Xiao, A.J. Kaufman, H. Bao, C. Zhou and H. Wang, Stratification and mixing of a post-glacial Neoproterozoic ocean: evidence from carbon and sulfur isotopes in a cap dolostone from northwest China, *Earth Planet. Sci. Lett.* **265** (2008), pp. 209–228.

Thompson and Bowring, 2000 M.D. Thompson and S.A. Bowring, Age of the Squantum "tillite", Boston Basin Massachusetts: U–Pb zircon constraints on terminal Neoproterozoic glaciation, *Am. J. Sci.* **300** (2000), pp. 630–655.

Williams and Claesson, 1987 I. Williams and S. Claesson, Isotopic evidence for the Precambrian provenance and Caledonian metamorphism of high-grade paragneisses from the Seve Nappes Scandinavian Caledonides. 2. Ion microprobe zircon U–Th–Pb, *Contrib. Miner. Petrol.* **97** (1987), pp. 205–217.

Xiao et al., 2004 S. Xiao, H. Bao, H. Wang, A.J. Kaufman, C. Zhou, G. Li, X. Yuan and H. Ling, The Neoproterozoic Quruqtagh Group in eastern Chinese Tianshan: evidence for a post-Marinoan glaciation, *Precambrian Res.* **130** (2004), pp. 1–26

Xing et al., 1984 Y. Xing, Q. Ding, H. Luo, T. He and Y. Wang, The Sinian–Cambrian Boundary of China. Bulletin of the Institute of Geology, *Chin. Acad. Geol. Sci.* **10** (1984), pp. 1–262.

Xu et al., 2003 B. Xu, H. Zheng, H. Yao and Y. Li, C-isotope composition and significance of the Sinian on the Tarim plate, *Chin. Sci. Bull.* **48** (4) (2003), pp. 385–389.

Xu et al., 2005 B. Xu, P. Jian, H. Zheng, H. Zou, L. Zhang and D. Liu, U–Pb zircon geochronology and geochemistry of Neoproterozoic volcanic rocks in the Tarim Block of northwest China: implications for the breakup of Rodinia supercontinent and Neoproterozoic glaciations, *Precambrian Res.* **136** (2) (2005), pp. 107–123.

Yao et al., 2005 J. Yao, S. Xiao, L. Yin, G. Li and X. Yuan, Basal Cambrian microfossils from the Yurtus and Xishanblaq formations (Tarim, north-west China): systematic revision and biostratigraphic correlation of *Micrhystridium*-like acritarchs from China, *Palaeontology* **48** (2005), pp. 687–708.

Yin et al., 2003 C. Yin, D. Liu, L. Gao, Z. Wang, Y. Xing, P. Jian and Y. Shi, Lower boundary age of the Nanhua System and the Gucheng glacial stage: evidence from SHRIMPII dating, *Chin. Sci. Bull.* **48** (16) (2003), pp. 1657–1662

Yin et al., 2005 C. Yin, F. Tang, Y. Liu, L. Gao, Z. Yang, Z. Wang, P. Liu, Y. Xing and B. Song, New U–Pb zircon ages from the Ediacaran (Sinian) System in the Yangtze Gorges:

Constraint on the age of Miaohe biota and Marinoan glaciation, *Geol. Bull. China* **24** (2005), pp. 393–400.

Zhang et al., 20
05 S. Zhang, G. Jiang, J. Zhang, B. Song, M.J. Kennedy and N. Christie-Blick, U–Pb sensitive high-resolution ion microprobe ages from the Doushantuo Formation in south China: constraints on late Neoproterozoic glaciations, *Geology* **33** (2005), pp. 473–476.

Zhao et al., 1980 Zhao, X., Zhang, L., Zou, X., Wang, S., Hu, Y., 1980. Sinian tillites in Northwest China and their stratigraphic significance. In: Tianjin Institute of Geology and Mineral Resources (Ed.), Research on Precambrian Geology Sinian Suberathem in China. Tianjin Science and Technology Press, Tianjin, pp. 164–185.

Zhou and Xiao, 2007 C. Zhou and S. Xiao, Ediacaran $\delta^{13}C$ chemostratigraphy of South China, *Chem. Geol.* **237** (2007), pp. 89–108.

Zhou et al., 2004 C. Zhou, R. Tucker, S. Xiao, Z. Peng, X. Yuan and Z. Chen, New constraints on the ages of Neoproterozoic glaciations in South China, *Geology* **32** (2004), pp. 437–440

# Figures

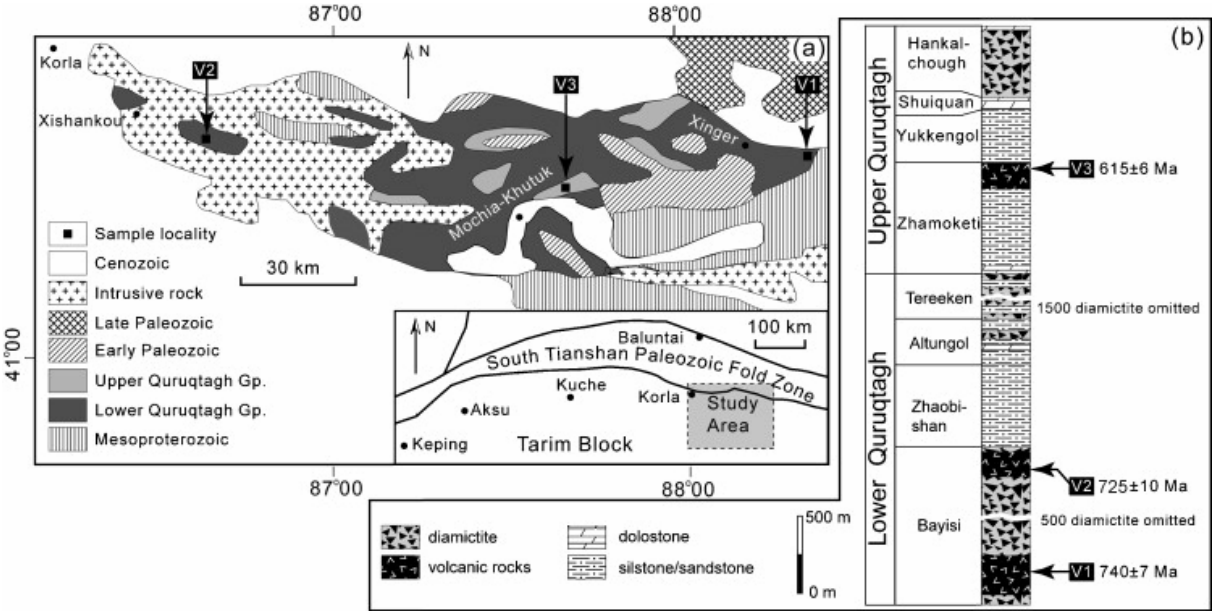


Fig. 1. Geological map of the Quruqtagh area (a) and stratigraphic column of the Quruqtagh Group (b). Inset in (a) shows major tectonic units of the Quruqtagh area. Sample localities and horizons are marked on the map and stratigraphic column.

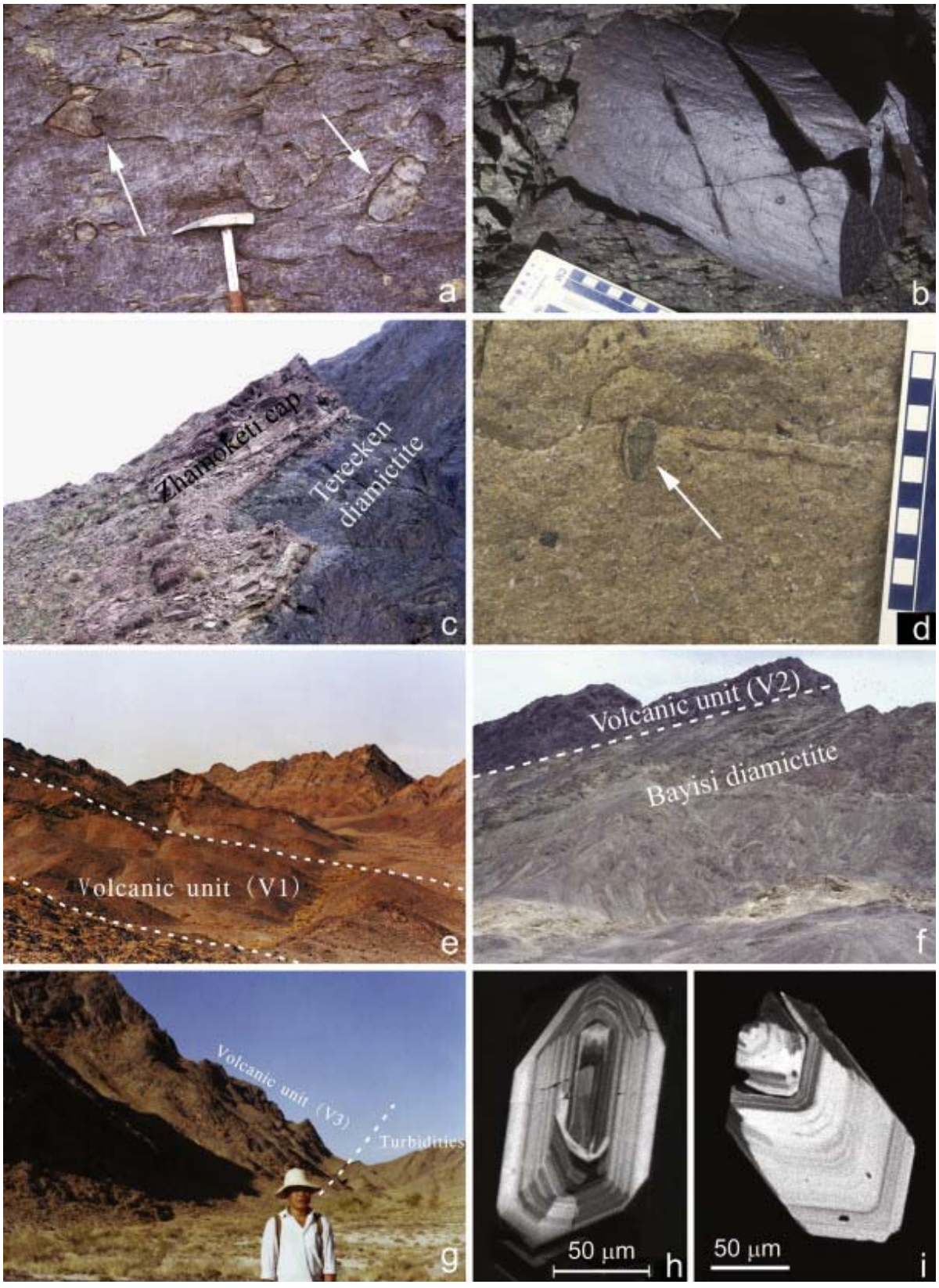


Fig. 2. Field photographs of outsized clasts (arrows) in Bayisi diamictite (a), a striated clast in Tereeken diamictite (b), Tereeken diamictite and overlying Zhamoketi cap carbonate (c), drop stone (arrow) in Hankalchough diamictite (d), volcanic interval V1 (e), volcanic interval V2 (f), volcanic interval V3 (g), and cathodoluminescence images of typical zircon crystals from V1 sample Xb006 (h) and from V3 sample 2371D (i).

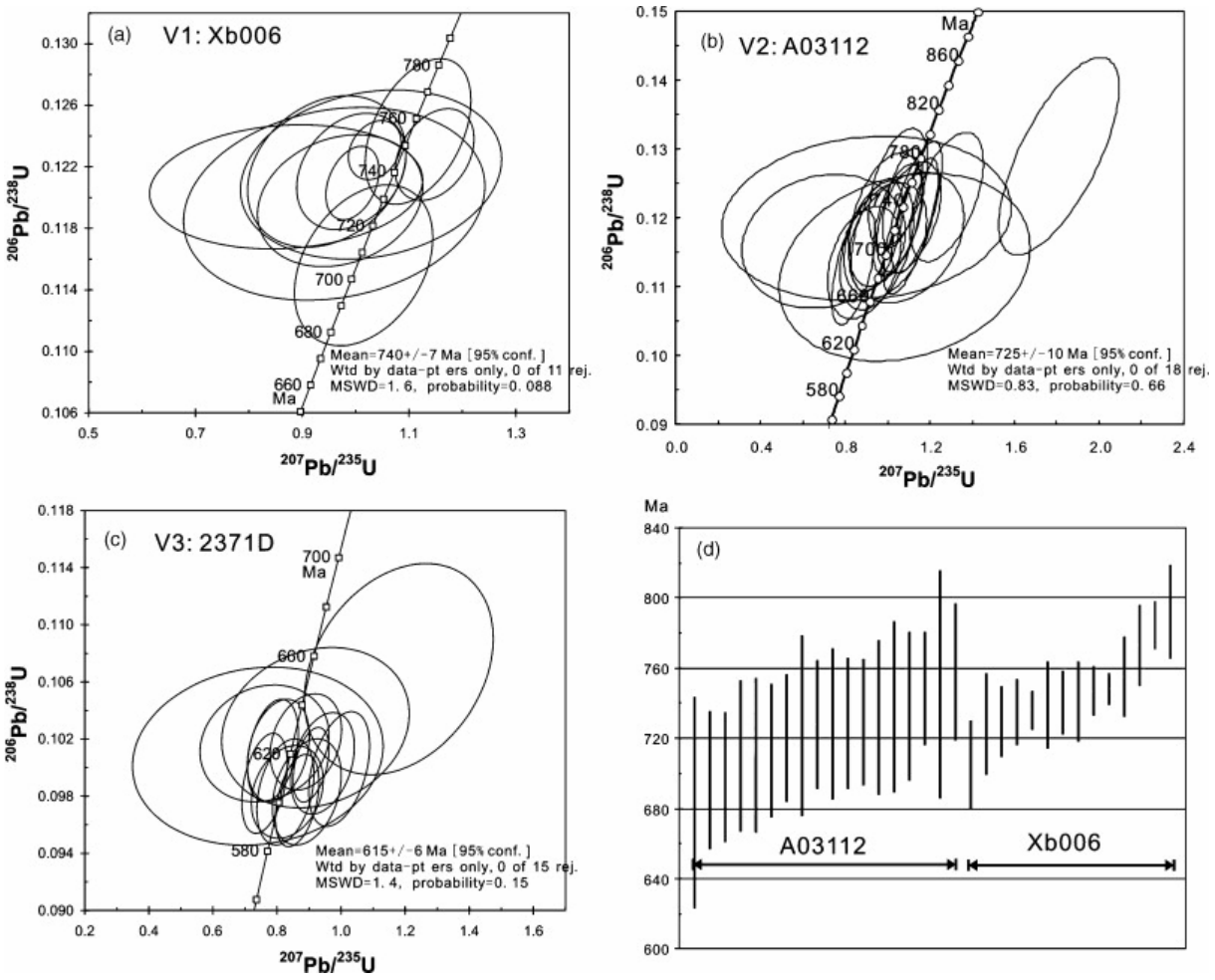


Fig. 3. (a–c) Concordia diagrams for volcanic samples analyzed in this study. MSWD: mean square of weighted deviates. Individual analyses in concordia plots are shown with 2$\sigma$ errors including the 2$\sigma$ errors for the means of the standard measurements (as in the tables). Uncertainty of mean ages was calculated at 95% confidence intervals. (d), $^{206}Pb/^{238}U$ ages of Xb006 (V1) and A03112 (V2) analyses. Error bars represent 2$\sigma$ errors with the 2$\sigma$ errors for the means of the standard measurements included (as in the tables). The three oldest 206/238 ages of sample Xb006, represented by gray bars, were not used in mean age calculation.

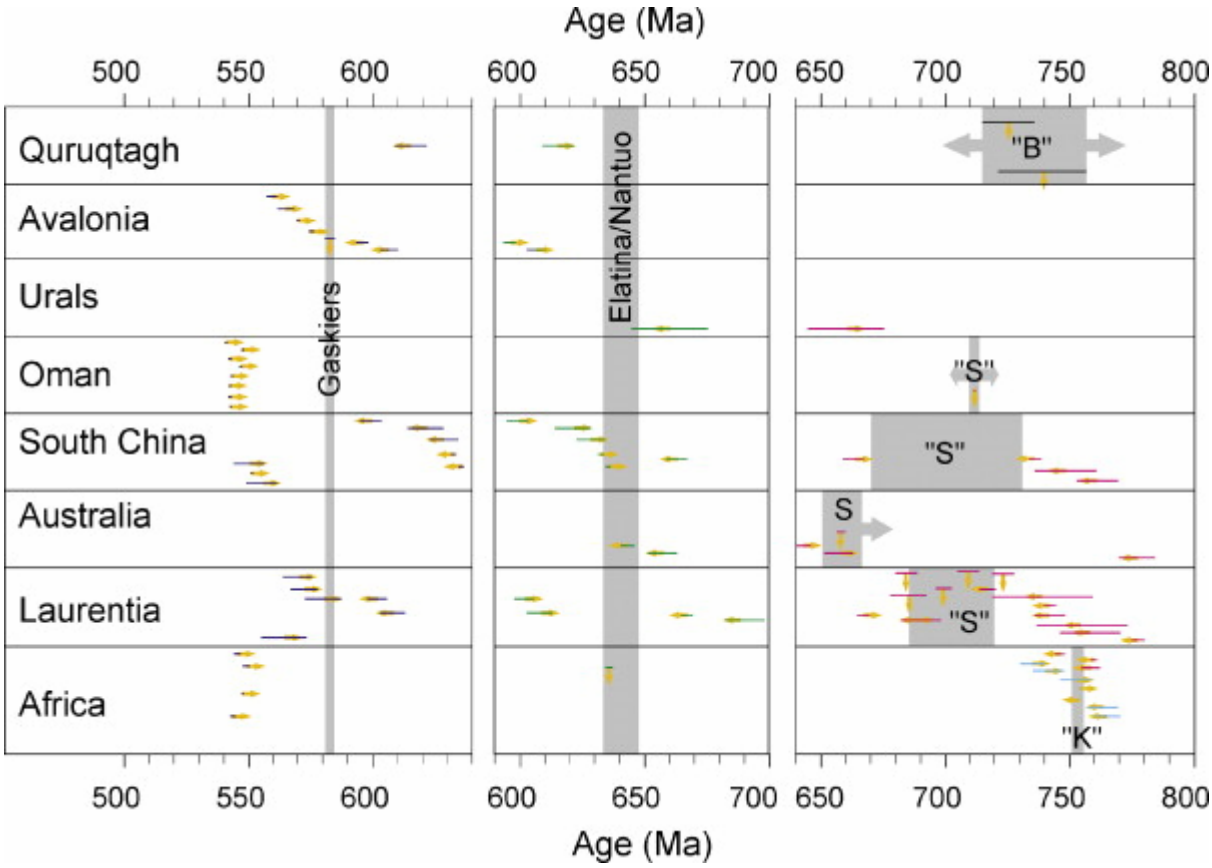


Fig. 4. U–Pb age constraints on Neoproterozoic glaciations. Data presentation follows Paul Hoffman (http://www.snowballearth.org), with left-pointing arrows representing maximum age constraints and right-pointing arrows representing minimum age constraints. Arrows pointing downward indicate syn-glacial ages. Age constraints are color coded: cyan, the Kaigas glaciation (“K”); black, Bayisi diamictite (“B”); pink, Sturtian glaciation (S) or presumed equivalents (“S”); green, Nantuo or Elatina glaciation, and blue, Gaskiers glaciation. Gray bars represent maximally allowed glaciation durations. The geochronometric data permit a globally synchronous Gaskiers glaciation and a globally synchronous Nantuo/Elatina glaciation, but require multiple glaciations or a long-lasting but globally diachronous glaciation (with diachronous initiation and termination) between ~750 Ma and ~650 Ma. See Table 4 for source of radiometric dates.

# Tables

Table 1. : SHRIMP U–Pb zircon data for sample Xb-006.

| Spot | % $^{206}Pb_c$ [b] | ppm U | ppm Th | $^{232}Th/^{238}U$ | ppm $^{206}Pb^*$ [b] | $^{206}Pb/^{238}U$ Age and 2σ error [a] | | $^{207}Pb^*/^{206}Pb^*$ and % error [a] | | $^{207}Pb^*/^{235}U$ and % error [a] | | $^{206}Pb^*/^{238}U$ and % error [a] | | Error correlation |
|---|---|---|---|---|---|---|---|---|---|---|---|---|---|---|
| Xb006-1. 1[c] | 4.83 | 188 | 26 | 0.15 | 21.6 | 773 | ±23 | 0.0572 | ±30% | 1.01 | ±30% | 0.1275 | ±3.1% | .102 |
| Xb006-2.1[c] | 1.48 | 117 | 110 | 0.98 | 13.3 | 792 | ±27 | 0.0603 | ±17% | 1.09 | ±18% | 0.1308 | ±3.5% | .190 |
| Xb006-3.1[c] | 0.59 | 201 | 102 | 0.53 | 64.4 | 2,035 | ±36 | 0.1401 | ±3.8% | 7.17 | ±4.3% | 0.3712 | ±2.0% | .434 |
| Xb006-4.1 | 1.39 | 92 | 36 | 0.41 | 9.76 | 741 | ±23 | 0.0564 | ±12% | 0.95 | ±13% | 0.1217 | ±3.3% | .254 |
| Xb006-5.1 | 1.42 | 57 | 48 | 0.87 | 5.97 | 728 | ±29 | 0.0582 | ±22% | 0.96 | ±24% | 0.1196 | ±4.3% | .181 |
| Xb006-6.1 | 3.72 | 207 | 52 | 0.26 | 22.3 | 735 | ±19 | 0.0524 | ±24% | 0.87 | ±24% | 0.1207 | ±2.7% | .111 |
| Xb006-7.1 | 1.18 | 142 | 140 | 1.02 | 14.8 | 730 | ±20 | 0.0588 | ±13% | 0.97 | ±13% | 0.1198 | ±2.9% | .208 |
| Xb006-8.1 | 1.33 | 83 | 14 | 0.17 | 8.34 | 705 | ±25 | 0.0636 | ±10% | 1.02 | ±10% | 0.1156 | ±3.7% | .343 |
| Xb006-9.1 | 0.88 | 181 | 122 | 0.70 | 19.1 | 740 | ±18 | 0.0591 | ±8.0% | 0.99 | ±8.4% | 0.1217 | ±2.5% | .282 |
| Xb006-10.1[c] | 0.81 | 397 | 22 | 0.06 | 44.5 | 785 | ±14 | 0.0624 | ±6.0% | 1.11 | ±6.3% | 0.1294 | ±1.9% | .265 |
| Xb006-11.1 | 0.33 | 623 | 60 | 0.10 | 64.9 | 736 | ±11 | 0.0596 | ±3.8% | 0.99 | ±4.1% | 0.1210 | ±1.6% | .341 |
| Xb006-12.1 | 1.57 | 91 | 9 | 0.10 | 9.64 | 739 | ±25 | 0.0614 | ±19% | 1.03 | ±19% | 0.1215 | ±3.7% | .183 |
| Xb006-13.1 | 1.09 | 2168 | 10 | 0.00 | 232 | 748 | ±9 | 0.0610 | ±3.6% | 1.04 | ±3.9% | 0.1231 | ±1.3% | .253 |
| Xb006-4.2 | 0.33 | 186 | 79 | 0.44 | 20.0 | 755 | ±23 | 0.0652 | ±6.6% | 1.12 | ±7.2% | 0.1243 | ±3.1% | .425 |
| Xb006-6.2 | 0.14 | 244 | 13 | 0.06 | 25.8 | 747 | ±14 | 0.0678 | ±5.0% | 1.15 | ±5.3% | 0.1228 | ±2.0% | .342 |

[a]Errors are 2$\sigma$; standard calibration errors included: 2$\sigma$ = SQRT [(2$\sigma$ error of a spot analysis)$^2$ + (2$\sigma$ error of weighted mean age for the standard)$^2$].

[b]$Pb_c$ and Pb* indicate the common and radiogenic portions, respectively. Common Pb corrected using measured $^{204}Pb$. 2$\sigma$ error in nine standard calibration was 0.84%.

[c]Data shown in gray are those rejected from mean-age calculation and are not shown in the concordia plot (Fig. 3).

Table 2. : SHRIMP U–Pb zircon data for sample A03112.

| Spot | % $^{206}Pb_c$ [b] | ppm U | ppm Th | $^{232}Th/^{238}U$ | ppm $^{206}Pb^*$ [b] | $^{206}Pb/^{238}U$ Age and 2σ error [a] | | $^{207}Pb^*/^{206}Pb^*$ and % error [a] | | $^{207}Pb^*/^{235}U$ and % error [a] | | $^{206}Pb^*/^{238}U$ and % error [a] | | Error correlation |
|---|---|---|---|---|---|---|---|---|---|---|---|---|---|---|
| A03112.1-1 | 0 | 53 | 50 | 0.98 | 5.6 | 738.2 | ±42.6 | .0752 | ±9.3% | 1.28 | ±10.9% | .1230 | ±5.9% | 0.544 |
| A03112.2-1 | 1.29 | 77 | 102 | 1.37 | 7.6 | 697.8 | ±37.1 | .0566 | ±14.8% | 0.89 | ±15.8% | .1135 | ±5.5% | 0.348 |
| A03112.3-1 | 1.63 | 48 | 56 | 1.21 | 4.8 | 710.3 | ±44.0 | .0596 | ±13.4% | 0.95 | ±14.8% | .1160 | ±6.3% | 0.425 |
| A03112.4-1 | 0.38 | 28 | 21 | 0.78 | 2.7 | 683.6 | ±60.1 | .0695 | ±43.8% | 1.08 | ±44.8% | .1128 | ±9.7% | 0.216 |
| A03112.5-1 | 1.48 | 61 | 73 | 1.23 | 6.4 | 731.9 | ±44.2 | .0600 | ±12.8% | 0.99 | ±14.2% | .1197 | ±6.3% | 0.442 |
| A03112.6-1 | 2.37 | 41 | 48 | 1.21 | 4.4 | 737.8 | ±48.7 | .0545 | ±61.6% | 0.90 | ±62.0% | .1199 | ±7.9% | 0.127 |
| A03112.7-1 [c] | 1.89 | 84 | 100 | 1.23 | 10.8 | 892.7 | ±55.3 | .0591 | ±31.4% | 1.20 | ±32.2% | .1468 | ±6.7% | 0.208 |
| A03112.8-1 | 1.74 | 102 | 133 | 1.36 | 10.0 | 696.3 | ±39.2 | .0538 | ±8.1% | 0.84 | ±9.9% | .1128 | ±5.7% | 0.579 |
| A03112.9-1 | 0.60 | 308 | 298 | 1.00 | 32.7 | 748.3 | ±32.2 | .0632 | ±5.5% | 1.07 | ±6.9% | .1229 | ±4.3% | 0.631 |
| A03112.10-1 | 0 | 20 | 16 | 0.81 | 2.2 | 750.7 | 64.9 | .1020 | ±9.3% | 1.81 | ±12.7% | .1289 | ±8.9% | 0.701 |
| A03112.11-1 [c] | 0.28 | 161 | 82 | 0.52 | 8.4 | 372.7 | ±19.2 | .0645 | ±6.3% | 0.54 | ±8.1% | .0603 | ±5.1% | 0.634 |
| A03112.12-1 | 0.00 | 59 | 69 | 1.22 | 6.0 | 727.1 | ±51.5 | .0675 | ±6.9% | 1.12 | ±9.9% | .1200 | ±7.3% | 0.739 |
| A03112.13-1 | 1.03 | 109 | 86 | 0.82 | 11.1 | 720.2 | ±36.6 | .0585 | ±8.9% | 0.95 | ±10.3% | .1175 | ±5.3% | 0.519 |
| A03112.14-1 | 0.71 | 104 | 139 | 1.38 | 11.2 | 757.9 | ±39.0 | .0615 | ±9.3% | 1.05 | ±10.7% | .1243 | ±5.3% | 0.499 |
| A03112.15-1 | 0 | 115 | 171 | 1.53 | 11.9 | 728.5 | ±37.2 | .0680 | ±5.7% | 1.13 | ±7.7% | .1203 | ±5.3% | 0.693 |
| A03112.16-1 | 0.69 | 89 | 114 | 1.32 | 9.0 | 713.0 | ±38.2 | .0613 | ±15.0% | 0.99 | ±16.0% | .1167 | ±5.5% | 0.344 |
| A03112.17-1 | 0.12 | 114 | 100 | 0.90 | 11.8 | 727.9 | ±36.6 | .0666 | ±9.9% | 1.10 | ±11.1% | .1200 | ±5.1% | 0.464 |
| A03112.18-1 | 0.39 | 126 | 173 | 1.42 | 13.0 | 729.0 | ±36.0 | .0633 | ±7.7% | 1.05 | ±9.1% | .1197 | ±5.1% | 0.565 |
| A03112.19-1 | 0.05 | 56 | 63 | 1.17 | 5.6 | 710.1 | ±43.2 | .0676 | ±19.2% | 1.09 | ±20.2% | .1171 | ±6.3% | 0.311 |
| A03112.20-1 | 3.02 | 58 | 70 | 1.25 | 6.0 | 728.4 | ±43.1 | .0435 | ±44.8% | 0.70 | ±45.2% | .1166 | ±6.5% | 0.144 |

[a]Errors are 2$\sigma$; standard calibration errors included: 2$\sigma$ = SQRT [(2$\sigma$ error of a spot analysis)$^2$ + (2$\sigma$ error of weighted mean age for the standard)$^2$].

[b]$Pb_c$ and Pb* indicate the common and radiogenic portions, respectively. 2$\sigma$ error for the standard mean was 1.13% based on 15 spot analyses. Common Pb corrected using measured $^{204}Pb$, but $^{206}Pb/^{238}U$ ages are after $^{207}Pb$ correction.

[c]Data shown in gray are those rejected from mean-age calculation and are not shown in the concordia plot (Fig. 3).

Table 3. : SHRIMP U–Pb zircon data for sample 2371D.

| Spot | % $^{206}Pb_c$ [b] | ppm U | ppm Th | $^{232}Th/^{238}U$ | ppm $^{206}Pb^*$ [b] | $^{206}Pb/^{238}U$ Age and 2σ error [a] | | $^{207}Pb^*/^{206}Pb^*$ and % error [a] | | $^{207}Pb^*/^{235}U$ and % error [a] | | $^{206}Pb^*/^{238}U$ and % error [a] | | Error correlation |
|---|---|---|---|---|---|---|---|---|---|---|---|---|---|---|
| 2371D-1.1 | 1.29 | 129 | 108 | 0.86 | 11.0 | 604 | ±17 | 0.0614 | ±11% | 0.832 | ±11% | 0.0983 | ±2.7% | .247 |
| 2371D-2.1 | 0.39 | 94 | 63 | 0.69 | 7.98 | 604 | ±19 | 0.0659 | ±9.0% | 0.893 | ±10% | 0.0983 | ±3.1% | .310 |
| 2371D-3.1 | 0.41 | 106 | 84 | 0.82 | 9.01 | 604 | ±17 | 0.0609 | ±8.0% | 0.826 | ±9.0% | 0.0983 | ±3.1% | .334 |
| 2371D-4.1 | 0.00 | 206 | 260 | 1.30 | 17.8 | 616 | ±13 | 0.0656 | ±4.6% | 0.906 | ±5.1% | 0.1002 | ±2.1% | .417 |
| 2371D-5.1 | 0.32 | 136 | 117 | 0.88 | 11.9 | 625 | ±17 | 0.0634 | ±10% | 0.890 | ±10% | 0.1018 | ±2.7% | .258 |
| 2371D-6.1 | 0.00 | 92 | 59 | 0.66 | 7.91 | 614 | ±19 | 0.0722 | ±7.2% | 0.994 | ±7.8% | 0.0999 | ±3.3% | .404 |
| 2371D-7.1 | 0.53 | 122 | 104 | 0.88 | 10.6 | 616 | ±17 | 0.0681 | ±8.0% | 0.942 | ±9.0% | 0.1003 | ±2.9% | .333 |
| 2371D-8.1 | 0.33 | 143 | 127 | 0.92 | 12.0 | 601 | ± 15 | 0.0641 | ±6.0% | 0.863 | ±6.4% | 0.0977 | ±2.7% | .396 |
| 2371D-9.1 | 2.35 | 54 | 29 | 0.56 | 4.87 | 631 | ±27 | 0.0650 | ±25% | 0.920 | ±26% | 0.1028 | ±4.5% | .174 |
| 2371D-10.1 [c] | 0.39 | 202 | 105 | 0.54 | 52.9 | 1,713 | ±33 | 0.1145 | ±2.8% | 4.80 | ±3.5% | 0.3044 | ±2.1% | .581 |
| 2371D-11.1 [c] | 0.43 | 90 | 60 | 0.68 | 22.8 | 1,655 | ±42 | 0.1127 | ±4.2% | 4.55 | ±5.3% | 0.2928 | ±2.9% | .533 |
| 2371D-12.1 [c] | 0.19 | 96 | 67 | 0.72 | 26.8 | 1,816 | ±41 | 0.1211 | ±3.0% | 5.43 | ±3.7% | 0.3254 | ±2.5% | .630 |
| 2371D-13.1 | 2.44 | 30 | 15 | 0.54 | 2.79 | 655 | ±36 | 0.0801 | ±19% | 1.18 | ±20% | 0.1069 | ±5.6% | .290 |
| 2371D-9.2 | 2.41 | 54 | 29 | 0.56 | 4.82 | 619 | ±28 | 0.0540 | ±44% | 0.740 | ±43% | 0.1008 | ±5.1% | .112 |
| 2371D-8.2 | 1.23 | 146 | 127 | 0.90 | 12.6 | 608 | ±17 | 0.0558 | ±7.2% | 0.761 | ±7.6% | 0.0989 | ±2.9% | .381 |
| 2371D-7.2 | 2.06 | 104 | 76 | 0.75 | 9.32 | 624 | ±19 | 0.0543 | ±21% | 0.761 | ±22% | 0.1017 | ±3.3% | .147 |
| 2371D-1.2 | 1.13 | 150 | 141 | 0.97 | 13.2 | 622 | ±17 | 0.0576 | ±9.4% | 0.804 | ±10% | 0.1012 | ±2.9% | .286 |
| 2371D-2.2 | 1.41 | 122 | 100 | 0.85 | 10.7 | 622 | ±17 | 0.0564 | ±7.4% | 0.787 | ±8.0% | 0.1012 | ±2.9% | .338 |

[a]Errors are 2$\sigma$; standard calibration errors included: 2$\sigma$ = SQRT [(2$\sigma$ error of a spot analysis)$^2$ + (2$\sigma$ error of weighted mean age for the standard)$^2$].

[b]$Pb_c$ and Pb* indicate the common and radiogenic portions, respectively. Common Pb corrected using measured $^{204}Pb$. 2$\sigma$ errors of means for 14 standard measurements was 0.73%.

[c]Data shown in gray are those rejected from mean-age calculation and are not shown in the concordia plot (Fig. 3).

Table 4.

Compilation of radiometric dates that are relevant to Neoproterozoic glaciations. Radiometric dates are tabulated as reported in the original literature. No corrections have been made with regard to decay constant, standard calibration, and trace calibration.

| **Geographic location** | **Age (Ma)** | **Uncertainty (+)** | **Uncertainty (−)** | **Description and stratigraphy** | **References** |
|---|---|---|---|---|---|
| Maximum ages for the Kaigas glaciation and presumed equivalents | | | | | |
| Africa | 765 | 5 | 5 | U–Pb SHRIMP maximum age for the Kundelungu glacial strata | Key et al. (2001) |
| Africa | 763 | 6 | 6 | U–Pb SHRIMP maximum age for the Kundelungu glacial strata | Key et al. (2001) |
| Africa | 754 | Not reported | Not reported | U–Pb TIMS Spitskop Volcanic Member (Stinkfontein Group) | Hoffmann et al. (2006) |
| | | | | | |
| Minimum ages for the Kaigas glaciation and presumed equivalents | | | | | |
| Africa | 752 | 6 | 6 | U–Pb SHRIMP felsic volcanic rocks above an older diamictite in the Port Nolloth Group in southern Namibia | Borg et al. (2003) |
| Africa | 741 | 6 | 6 | U–Pb TIMS Kalahari Craton; above Kaigas diamictite | Frimmel et al. (1996) |
| Africa | 735 | 5 | 5 | U–Pb SHRIMP Katanga Supergp, Zambia; above “Kaigas” diamictite | Key et al. (2001) |
| Africa | | Not reported | Not reported | U–Pb TIMS Rosh Pinah (Hilda Subgroup, lower Port Nolloth Group) | Hoffmann et al. (2006) |

| Geographic location | Age (Ma) | Uncertainty (+) | Uncertainty (−) | Description and stratigraphy | References |
|---|---|---|---|---|---|
| | 754 | | | | |
| | | | | | |
| Ages from within the Bayisi diamictite | | | | | |
| Quruqtagh | 740 | 7 | 7 | U–Pb SHIRMP Bayisi; within Bayisi diamictite | This paper |
| Quruqtagh | 725 | 10 | 10 | U–Pb SHIRMP Bayisi; within Bayisi diamictite | This paper |
| | | | | | |
| Maximum ages for the “Sturtian” glaciation | | | | | |
| Laurentia | 777 | 3 | 2 | U–Pb TIMS Little Dal Group; below the Rapitan Group | Jefferson and Parrish (1989) |
| Australia | 777 | 7 | 7 | U–Pb SHRIMP Boucat Volcanics South Australia | Preiss (2000) |
| South China | 761 | 8 | 8 | U–Pb SHRIMP Danzhou Gp below Chang’an diamictite | Li et al. (2003) |
| Africa | 760 | 1 | 1 | U–Pb TIMS Otavi Gp; below Chuos diamictite | Halverson et al. (2005) |
| Africa | 758.5 | 3.5 | 3.5 | U–Pb TIMS Ombombo Subgp, Otavi Gp; below Chuos diamictite | Hoffman et al. (1996) and Hoffman et al. (1998a) |
| Laurentia | 758 | 12 | 12 | U–Pb TIMS Mount Rogers Formation; below Konnarock diamictite | Aleinikoff et al. (1995) |

| Geographic location | Age (Ma) | Uncertainty (+) | Uncertainty (−) | Description and stratigraphy | References |
|---|---|---|---|---|---|
| South China | 758 | 23 | 23 | U–Pb SHRIMP Xieshuihe Fm; interpreted to be below the Chang'an diamictite | Yin et al. (2003) |
| Laurentia | 755 | 18 | 18 | U–Pb TIMS of granitic clast in Sayunei Formation of Rapitan Group | Ross and Villeneuve (1997) |
| South China | 748 | 12 | 12 | U–Pb SHRIMP Liantuo Formation; interpreted to be below the Chang'an diamictite | Ma et al. (1984) |
| Africa | 746 | 2 | 2 | U–Pb TIMS Congo Craton; below Chuos diamictite | Hoffman et al. (1996) |
| Laurentia | 742 | 6 | 6 | U–Pb TIMS Kwagunt Formation; below Sixty Miles Formation | Karlstrom et al. (2000) |
| Laurentia | 742 | 2 | 2 | U–Pb TIMS rhyolitic flow below diamictite in the Grandfather Mountain Formation | Fetter and Goldberg (1995) |
| Laurentia | 736 | 23 | 17 | U–Pb TIMS of youngest magmatic unit in basement of Toby Formation | McDonough and Parrish (1991) |
| South China | 736 | 2 | 2 | U–Pb TIMS Keratophyre tuff Banxi Group; below Chang'an diamictite | Gan et al. (1993) |
| Laurentia | 717 | 4 | 4 | U–Pb SHRIMP clast in Scout Mountain diamictite | Fanning and Link (2004) |
| | | | | | |
| Ages from within "Sturtian" diamictites | | | | | |
| Laurentia | 723 | 4 | 4 | U–Pb TIMS baddeleyite of Franklin dikes which has coincident | Heaman et al. |

| Geographic location | Age (Ma) | Uncertainty (+) | Uncertainty (−) | Description and stratigraphy | References |
|---|---|---|---|---|---|
| | | | | paleopoles w/Sayunei Fm | (1992) |
| Oman | 711.5 | 0.3 | 0.3 | U–Pb TIMS Ghubrah diamictite | Bowring et al. (2007) |
| Lauerentia | 709 | 4 | 4 | U–Pb SHRIMP Bancock Volcanic Member; interpreted as synglacial | Fanning and Link (2004) |
| Lauerentia | 699 | 3 | 3 | U–Pb SHRIMP Rhyolite from pendant in Idaho bathlith (Big Creek) | Evans et al. (1997) |
| Lauerentia | 685 | 7 | 7 | U–Pb SHRIMP Rhyodacite flow Edwardsburg Fm | Lund et al. (2003) |
| Lauerentia | 684 | 4 | 4 | U–Pb SHRIMP Rhyodacite flow Edwardsburg Fm | Lund et al. (2003) |
| Australia | 658 | Not reported | Not reported | U–Pb SHRIMP Merinjina Formation | Fanning and Link (2006) |
| | | | | | |
| Ages between “Sturtian” and Marinoan diamictites | | | | | |
| Laurentia | 688.6 | 9.5 | 6.2 | U–Pb TIMS felsic volcaniclastic Gataga Mountains, N. B. C. possibly correlative with Hyland Group in Yukon | Ferri et al. (1999) |
| Laurentia | 667 | 2 | 2 | U–Pb SHRIMP Upper Scout Mountain Member; above Scout Mountain diamictite | Fanning and Link (2004) |
| South China | 663 | 4 | 4 | U–Pb TIMS Datangpo Formation, below Nantuo diamictite and above Tiesiao diamictite | Zhou et al. (2004) |
| Urals | 660 | 15 | 15 | U–Pb TIMS Urals, below Laplandian diamictite | Semikhatov (1991) |

| Geographic location | Age (Ma) | Uncertainty (+) | Uncertainty (−) | Description and stratigraphy | References |
|---|---|---|---|---|---|
| Australia | 657.2 | 5.4 | 5.4 | Re–Os isochron Aralka Formation, central Australia | Kendall et al. (2006) |
| Australia | 643 | 2.4 | 2.4 | Re–Os isochron Tindelpina Member, Adelaide Rift | Kendall et al. (2006) |
| Australia | 592 | 14 | 14 | Re–Os isochron Aralka Formation, central Australia | Schaefer and Burgess (2003) |
| | | | | | |
| Age from within Marinoan diamictites | | | | | |
| Africa | 635.5 | 1.2 | 1.2 | U–Pb TIMS Swakop Group central Namibia | Hoffmann et al. (2004) |
| | | | | | |
| Minimum ages for the Marinoan glaciation or ages between Marinoan and Gaskiers diamictites | | | | | |
| South China | 635.2 | 0.6 | 0.6 | U–Pb TIMS lower Doushantuo, above Nantuo diamictite | Condon et al. (2005) |
| South China | 632.5 | 0.5 | 0.5 | U–Pb TIMS lower Doushantuo, above Nantuo diamictite | Condon et al. (2005) |
| South China | 628.3 | 5.8 | 5.8 | U–Pb TIMS lower Doushantuo, above Nantuo diamictite | Yin et al. (2005) |
| South China | 621 | 7 | 7 | U–Pb SHRIMP Doushantuo, above Nantuo diamictite | Zhang et al. (2005) |
| Quruqtagh | 615 | 6 | 6 | U–Pb SHRIMP Zhamoketi, above Tereeken diamictite, below Hankalchough diamictite | This paper |

| Geographic location | Age (Ma) | Uncertainty (+) | Uncertainty (−) | Description and stratigraphy | References |
|---|---|---|---|---|---|
| Laurentia | 607.8 | 4.7 | 4.7 | Re–Os isochron Old Fort Point Fm | Kendall et al. (2004) |
| Avalonia | 606 | 3.7 | 2.9 | U–Pb TIMS Harbour Main Group; below Gaskiers diamictite | Krogh et al. (1988) |
| Laurentia | 601.4 | 3.7 | 3.7 | U–Pb SHRIMP Tayvallich volcanics | Dempster et al. (2002) |
| South China | 599 | 4 | 4 | Pb–Pb isochron Doushantuo Formation; above Nantuo diamictite; | Barfod et al. (2002) |
| Avalonia | 595.5 | 2 | 2 | U–Pb TIMS tuff clast in Squantum diamictite | Thompson and Bowring (2000) |
| Australia | 582 | 4 | 4 | U–Pb SHRIMP Togari Group Rhyodacite flow below Croles Hill diamictite. The Croles Hill diamictite was interpreted by the original authors as equivalent to the Marinoan glaciation. If so, this date provides a maximum age for the Marinoan glaciation. Because the Croles Hill diamictite may represent a Gaskiers-age diamictite, we tentatively interpret the 582 ± 4 Ma age as a maximum age constraint for the Gaskiers glaciation. | Calver et al. (2004) |
| Australia | 575 | 3 | 3 | U–Pb SHRIMP Grimes Intrusive Suite Cutting Cotton Breccia in King Island. | Calver et al. (2004) |
| | | | | | |
| Age from within Gaskiers diamictites | | | | | |
| Avalonia | 582 | 1 | 1 | U–Pb TIMS Gaskiers diamictite | Bowring et al. (2003) |

| Geographic location | Age (Ma) | Uncertainty (+) | Uncertainty (−) | Description and stratigraphy | References |
|---|---|---|---|---|---|
| | | | | | |
| Minimum ages for the Gaskiers glaciation | | | | | |
| Laurentia | 580 | 7 | 7 | Ar–Ar hbl Trachyte Browns Hole Fm, Brigham Gp, N. Utah | Link et al. (1993) |
| Avalonia | 575 | 1 | 1 | U–Pb TIMS Drooks Formation; above Gaskiers diamictite | Bowring et al. (2003) |
| Laurentia | 572 | 5 | 5 | U–Pb TIMS dike presumed to feed Catoctin flow | Aleinikoff et al. (1995) |
| Avalonia | 570 | | | U–Pb TIMS youngest detrital zircon in the Cambridge Argillite | Thompson and Bowring (2000) |
| Laurentia | 569.6 | 5.3 | 5.3 | U–Pb TIMS Tachy-andesite from Hamill Group, SE B.C. | Colpron et al. (2002) |
| Avalonia | 565 | 3 | 3 | U–Pb TIMS Mistaken Point Fm; above Gaskiers diamictite | Benus (1988) |
| Laurentia | 564 | 9 | 9 | U–Pb TIMS Catoctin flow | Aleinikoff et al. (1995) |
| Avalonia | 559.3 | 2 | 2 | U–Pb SHRIMP Beacon Hill Formation of Charnian Supergroup | Compston et al. (2002) |
| Russia | 555.3 | 0.3 | 0.3 | U–Pb TIMS White Sea Ediacaran Fossils | Martin et al. (2000) |
| South China | 555.2 | 6.1 | 6.1 | U–Pb SHRIMP upper Doushantuo | Zhang et al. (2005) |
| South China | 551.1 | 0.7 | 0.7 | U–Pb TIMS upper Doushantuo | Condon et al. |

| Geographic location | Age (Ma) | Uncertainty (+) | Uncertainty (−) | Description and stratigraphy | References |
|---|---|---|---|---|---|
| | | | | | (2005) |
| South China | 549.9 | 6.1 | 6.1 | U–Pb SHRIMP upper Doushantuo | Yin et al. (2005) |
| Africa | 547.4 | 0.3 | 0.3 | U–Pb TIMS Namibia | Bowring et al. (2007) |
| Africa | 545.1 | 1 | 1 | U–Pb TIMS Namibia | Grotzinger et al. (1995) |
| Africa | 543.3 | 1 | 1 | U–Pb TIMS Namibia | Grotzinger et al. (1995) |
| Oman | 542.3 | 0.2 | 0.2 | U–Pb TIMS; Ara Group Oman, *Cloudina* | Bowring et al. (2007) |
| Oman | 542.9 | 0.2 | 0.2 | U–Pb TIMS; Ara Group Oman, *Cloudina* | Bowring et al. (2007) |
| Oman | 546.7 | 0.3 | 0.3 | U–Pb TIMS; Ara Group Oman, *Cloudina* | Bowring et al. (2007) |
| Oman | 542.5 | 0.5 | 0.5 | U–Pb TIMS; Ara Group Oman, *Cloudina* | Bowring et al. (2007) |
| Oman | 547.2 | 0.4 | 0.4 | U–Pb TIMS; Ara Group Oman, *Cloudina* | Bowring et al. (2007) |
| Oman | 541 | 0.2 | 0.2 | U–Pb TIMS; Ara Group Oman, *Cloudina* | |